SIMULATION CALCULATION OF FLUID FIELD- THERMAL FIELD OF OIL-IMMERSED TRANSFORMER AND OPTIMIZATION OF WINDING STRUCTURE PARAMETERS

FaTing YUAN[1,2], BoYuan KUANG[1], NaiYue ZHANG[1], LingYun GU[3], YuQing JIANG[1], Bo TANG[1,2]

[1] College of Electrical Engineering and New Energy, China Three Gorges University, Yichang, China

[2] Hubei Provincial Engineering Technology Research Center for Power Transmission Line, China Three Gorges University, Yichang, China

[3] Beijing Key Laboratory of Distribution Transformer Energy-Saving Technology (China Electric Power Research Institute)

Corresponding author: E-mail: yuanfatinghss@163.com

The optimization method of winding structure parameters of oil-immersed transformer is proposed to reduce the hot spot temperature of transformer and the metal conductor consumption based on the coupling calculation method of electromagnetic-fluid-thermal. Firstly, according to the electrical and structural parameters of the oil-immersed transformer, a 3D simulation model is established by using finite element software, and the distribution of the thermal field and the fluid field around the transformer as well as the fluid field and thermal field of the low-voltage winding are obtained. In order to accurately reflect the temperature rise distribution characteristics of the low-voltage winding, a 2D model of the low-voltage winding of the transformer was established considering the calculation efficiency and accuracy, and the thermal field and fluid field distribution of the two low-voltage winding models were compared and analyzed. The temperature error was less than 5.98℃, which verified the accuracy of the equivalent model. On this basis, the hot spot temperature of low voltage winding under different structural parameters is obtained by combining the Latin hypercube experiment design and thermal field simulation method, and the response surface model of winding hot spot temperature and structural parameters is established. Taking the hot spot temperature of low voltage winding and the amount of metal conductor as optimization objectives, combined with the response surface model, the optimal solution set of Pareto is obtained by using NSGS-Ⅱ optimization algorithm, and two kinds of optimal design results are obtained on the Pareto front surface. The results show that the hot spot temperature is reduced by 4.16% and the metal conductor consumption is reduced by 13.79% in scheme 1; the hot spot temperature is reduced by 0.51% and the metal conductor consumption is reduced by 28.46% in scheme 2. The research results have important guiding significance for the optimization of oil-immersed transformer.

Key words*: Oil-immersed transformer; Metal conductor usage; fluid-thermal coupling; Winding structure parameters; Response surface methodology*

1. Introduction

As an important equipment in power system, the oil-immersed transformer plays a key role in the stability of the system. The characteristics of high voltage level and large capacity cause the temperature rise problem to become increasingly serious, and too high temperature rise will not only accelerate the aging of insulation, but also induce damage or even destruction of winding insulation. At present, the temperature rise is reduced by increasing the cross section of the conductor, but this method inevitably leads to a significant increase in the amount of metal used. In order to take into account the metal conductor consumption and hot spot temperature rise of oil-immersed transformer, it is very important to carry out multi-physical coupling calculation and optimization of winding structure parameters of oil-immersed transformer.

In terms of hot spot temperature calculation, at present, the calculation methods for hot spot temperature rise of transformers mainly include empirical formula method [1], hot path model method [3-5] and numerical simulation method [6-8], but these three methods all have their drawbacks. Hu Wanjun et al. adopted the steady-state temperature rise and order reduction calculation method and established the order reduction model based on the basic principles of eigenorthogonal decomposition algorithm and discrete empirical interpolation algorithm [9]. Luo Rensong et al. built a three-dimensional thermal model of a high-power high-frequency transformer based on the finite difference method and analyzed the discretization error and its governing equation [10]. Lu Jinhan et al. proposed to combine the theory of porous media with the oil-immersed transformer to build a simplified model and verify its accuracy [11]. Literature [12] proposes a hybrid algorithm for heterogeneous grid node data mapping, which can accurately map electromagnetic losses to the fluid-temperature field. However, the actual structure of the medium oil immersed transformer is complex, and the existing method can not take both accuracy and efficiency into account in the numerical calculation process, which makes it difficult to accurately calculate the hot spot temperature of the transformer winding.

In terms of transformer temperature optimization, literature [13] studied the relationship between the inlet flow of a high-oil circulating transformer and the flow velocity of each oil passage inside the transformer, and proposed an optimization method to reduce the inlet oil temperature to reduce the temperature rise inside the transformer. Huang Jia et al. analyzed the influence of oil flow in horizontal oil passage on winding temperature rise, analyzed the improvement effect of adding oil baffle on reducing winding hot spot temperature, and proposed an optimization method for reducing winding hot spot temperature with two kinds of oil baffle structures [14]. Literature [15] analyzed the effects of inlet velocity of oil-immersed transformer, horizontal passage width and pie winding zone number on oil flow velocity and winding temperature rise, and proposed an optimization method to reduce hot spot temperature by changing structural parameters. However, the whole structure of oil-immersed transformer has many variables, and involves many constraints and multiple objectives. The above method has the problem of long optimization time and easy to fall into the local optimal solution, which limits its practical application.

According to the electrical and structural parameters of the oil-immersed transformer, the multi-physics coupling calculation of the three-dimensional model of the transformer is carried out, and the

distribution of the temperature field and flow field of the transformer is obtained. A two-dimensional transformer model is established, and the temperature field and flow field distribution of the two low-voltage winding models are compared and analyzed. The hot spot temperature error of the winding is only 5.98%, which verifies the accuracy of the equivalent model. The response relation between hot spot temperature and structural parameters is established by response surface method, and the Pareto algorithm is used to optimize the hot spot temperature and conductor quantity. The optimization method can significantly reduce the metal conductor quantity and hot spot temperature, which has important guiding significance for the design of oil-immersed transformer.

2. The Basic Structure and Equivalent Model of Transformer

2.1. The basic structure and parameters of transformer

The research object of this paper is three-phase oil-immersed transformer, and its main electrical parameters are shown in Table 1. The core components of the transformer are the iron core and the winding, the iron core is composed of cold rolled silicon steel sheets stacked together, the winding is divided into high voltage and low voltage winding, concentrically wound on the core column. The tank is filled with transformer oil, which acts as insulation and heat dissipation. The upper and lower collector tubing and heat sink constitute the heat dissipation system of the transformer, and realize the circulation cooling of the oil.

Table 1 Main Electrical Parameters of Transformers

Parameter	Value (Model)
Model	SZ11-10000/35
Rated capacity	240000kVA
Rated frequency	50Hz
Connection group	YNd11
Cooling method	ONAH
Rated voltage	220kV

2.2. Transformer Equivalent Model

According to the actual structural parameters of the oil-immersed transformer, the three-dimensional equivalent modeling of the transformer is carried out by using simulation software. The main parameters of transformer are: The height of the core is 1160mm, the depth is 240mm, the width is 2500mm, the inner radius of the low pressure winding is 305mm, the outer radius is 359mm, the inner radius of the high pressure winding is 420mm, the outer radius is 480mm, the width of the fuel tank is 3800mm, the depth is 1350mm, the height is 1825mm.

Considering the complex internal structure of the oil-immersed transformer, in order to save calculation time, the model is simplified as follows:

1) The winding is equivalent to a completely symmetrical cylinder type, without considering the effect of winding insulation on heat transfer and heat dissipation.

2) Ignoring the losses in structural parts such as clamps, pads and high voltage windings, and the heat source includes the loss of iron core and low voltage windings.

3) The structure of the heat sink and the shape of the oil passage are simplified and replaced by

cuboid sheets.

4) Baffles are set inside and outside the low-voltage winding and the oil passage to change the direction of oil flow.

The 3D equivalent model of the oil-immersed transformer and its internal structure are shown in Fig. 1 and Fig. 2. The winding coils are divided into three phases: A, B and C.

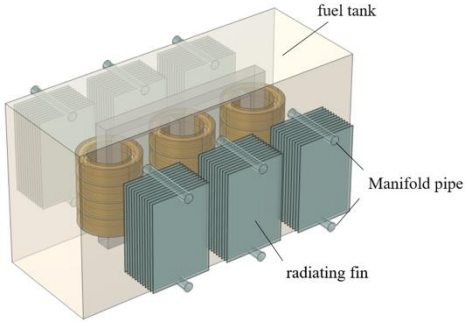

Figure 1. 3D equivalent model of transformer

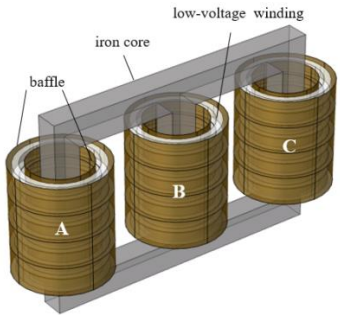

Figure 2. Internal Structure of Transformer

3. Simulation results of 3D temperature field of oil-immersed transformer

3.1. Heat transfer analysis and governing equation

3.1.1 Analysis of transformer heat transfer process

The research object of this paper is oil-immersed self-cooled transformer, whose heat transfer process is divided into three forms: heat conduction, heat convection and heat radiation. When the transformer is running, the loss of each component increases the outer surface temperature of the component through heat transfer. The heat transfer process of the oil-immersed transformer is shown in Fig. 3.

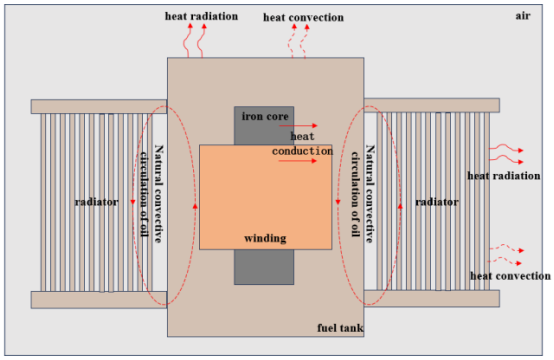

Figure 3. Heat transfer process of oil-immersed transformer

3.1.2 Governing equation

1) Magnetic field governing equation

In the normal operation of the oil-immersed transformer, the coil power leads to the loss of the core and winding and other structural parts, which as a heat source makes the temperature of the transformer core and winding rise gradually. The loss generated by the transformer mainly comes from the loss generated by the inner core and the loss generated by the winding, and the loss is closely related to the distribution of the magnetic flux density inside the core. Therefore, it is necessary to

solve the transformer magnetic field first, and the transformer governing equation based on vector magnetic potential A is as follows:

$$\nabla \frac{1}{\mu}(\nabla \times \vec{A}) = \overrightarrow{J_s} - \sigma \frac{\partial \vec{A}}{\partial t} \tag{1}$$

Where μ is the magnetic permeability, the unit is H/m, σ is the electrical conductivity, the unit is S/m; $\overrightarrow{J_s}$ is the current density of the winding, expressed in A/m^2.

2) fluid-thermal field governing equation

Numerical problems of fluid flow and heat transfer need to follow the law of conservation of mass, momentum and energy, where the governing equation describing the conservation of fluid momentum is also called the Navier-Stokes equation. Transformer oil is in a natural circulation state, the oil flow velocity is low, and the corresponding Reynolds number is small, so it is regarded as laminar flow, and its governing equation is as follows:

$$\frac{\partial \rho_0}{\partial t} + \nabla(\rho_0 v) = 0 \tag{2}$$

$$\rho_0 \frac{\delta v}{\delta t} + \rho_0 v \cdot \nabla v = -\nabla p + \mu_0 \nabla^2 v + F \tag{3}$$

$$\rho_0 c_p \frac{\delta T}{\delta t} + \rho_0 c_p v \cdot \nabla \mathrm{T} = \nabla \cdot (\mathrm{k} \nabla \mathrm{T}) - p \nabla v + Q \tag{4}$$

Where ρ_0 is the fluid density; v is the velocity; p is fluid pressure; μ_0 is hydrodynamic viscosity; F is the external force per unit volume; g is the degree of gravitational acceleration; c_p is the heat capacity at constant pressure; T is the temperature; k is thermal conductivity; Q is the internal heat source per unit volume; ∇ is the Hamiltonian operator.

3) Solid heat conduction equation

The heat transfer between solids is generally heat conduction. In the heat transfer process inside the oil-immersed transformer, due to the influence of uneven loss, the temperature difference is caused in the core and high and low voltage windings. At this time, the heat is mainly transferred to the surface of the medium through heat conduction, and then the heat is transferred through the transformer oil. Heat conduction follows Fourier's law, and its three-dimensional temperature field heat conduction equation is as follows:

$$\rho c \frac{\partial T}{\partial t} = \nabla(\lambda \nabla T) + q \tag{5}$$

Where, q is the heat source density of structural parts, ρ is the solid density; c is the heat capacity at constant pressure; λ is the thermal conductivity; T is temperature.

4) The expressions of loss

Transformer loss is mainly composed of core loss and winding loss. Core loss is calculated as follows:

$$Q_c = k_h f^{\alpha} B_m^{\beta} \tag{6}$$

Where Q_c is the core loss density; f is the excitation signal frequency; B_m is the peak magnetic induction intensity; k_h, α and β are loss coefficients.

The winding loss is calculated as follows:

$$Q_i = I_i^2 \frac{\pi D_i W_i}{k S_i} \tag{7}$$

Where, Q_i is winding loss; I_i, D_i, W_i and S_i are the current value, diameter, turns and cross-sectional area of the wire respectively, and k is the conductivity of the metal conductor.

3.2. Material properties and boundary conditions

Setting the material properties for the main components of the oil-immersed transformer, as shown in Table 2, where the core and winding add silicon steel sheet and copper, respectively, and the fluid material in the fuel tank and radiator is transformer oil. The coupling calculation of transformer fluid-thermal field is largely affected by the thermophysical properties of oil, so the thermophysical properties of transformer oil are set as a relation with temperature, where T is in Kelvin (K).\

Tab.2 Material property parameters

Material	Features	Value
Winding (copper)	thermal conductivity /($W \cdot m^{-1} \cdot K^{-1}$)	400
	specific heat capacity /($J \cdot kg^{-1} \cdot K^{-1}$)	385
	density /($kg.m^{-3}$)	8940
Iron core (silicon steel)	thermal conductivity /($W \cdot m^{-1} \cdot K^{-1}$)	72
	specific heat capacity /($J \cdot kg^{-1} \cdot K^{-1}$)	446
	density /($kg.m^{-3}$)	7550
Transformer oil	thermal conductivity /($W \cdot m^{-1} \cdot K^{-1}$)	$0.134-8.05\times10^{-5}T$
	specific heat capacity /($J \cdot kg^{-1} \cdot K^{-1}$)	$-13408.15+123.04T-0.33T^2$
	density /($kg.m^{-3}$)	$1055.05-0.58T-6.4\times10^{-5}T^2$
	dynamic viscosity /(Pa·s)	$91.45-1.33T+7.78\times10^{-3}T^2-2.27\times10^{-5}T^3$

The boundary conditions are set as follows:

(1) Heat conduction boundary conditions

$$q = \lambda \cdot \frac{\Delta T}{L} \tag{8}$$

Where, q is the heat flux per unit area, λ is the thermal conductivity, ΔT is temperature difference, L is the thickness.

(2) heat radiation

$$q = \varepsilon\beta(T_1^4 - T_2^4) \tag{9}$$

Where, ε is the radiation blackness, β is the Boltzmann constant, and T_1 and T_2 are the surface temperatures of the transformer and the air temperature respectively.

(3) heat convection

$$\begin{cases} h(T_\alpha - T_s) + \lambda \dfrac{\delta T}{\delta x} = 0 \\ h(T_\alpha - T_s) + \lambda \dfrac{\delta T}{\delta \mathrm{y}} = 0 \\ h(T_\alpha - T_s) + \lambda \dfrac{\delta T}{\delta z} = 0 \end{cases} \tag{10}$$

Where, h is the convective heat transfer coefficient, T_α solid boundary temperature, T_s is the fluid temperature, and λ is the thermal conductivity.

According to the heat transfer process of the transformer, convective heat transfer occurs between the outer surface of the fuel tank and the heat sink and the outside air. The calculated

convective heat transfer coefficients of each surface are shown in Table 3. The initial temperature T_0 and room temperature were set to 298.15K, the initial oil flow velocity v_0 was set to zero, and there was no slip on the fluid wall. Gravity is included in the calculation of fluid field, and its value is 9.8 m/s^2. The boundary condition diagram is shown in Fig. 4.

Tab.3 Convective heat transfer coefficient on the surface of transformer

Position	Tank top	Tank side	Tank bottom	Heat sink
$h/(W\cdot m^{-2}\cdot K^{-1})$	4.0	6.0	3.3	9.6

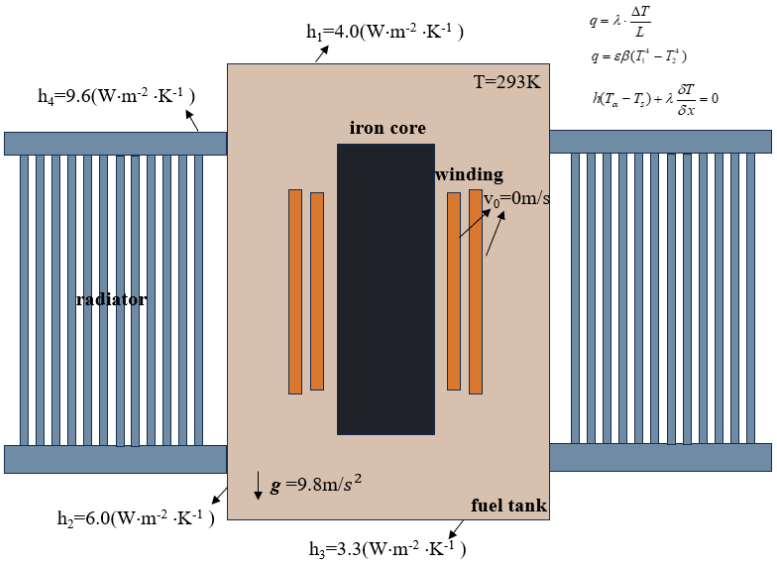

Figure.4 Boundary condition schematic diagram

3.3. Calculation of equivalent thermal parameters of low voltage winding

In order to take into account the calculation accuracy and efficiency, the thermal conductivity and specific heat capacity of low-voltage winding of oil-immersed transformer are equivalent.

3.3.1 Calculation of equivalent thermal conductivity

The thermal parameters of the wire and the insulating paper are equivalent, and the simplified diagram of the winding structure is shown in Fig. 5. In the figure, x and y represent radial and axial directions respectively. *H* and *d* are height and thickness respectively. The equivalent thermal conductivity of transformer winding in axial and radial direction can be obtained by equivalent thermal resistance model.

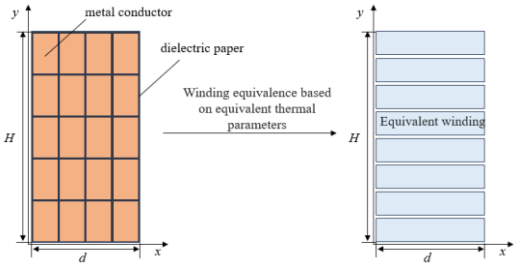

Figure.5 Simplified schematic diagram of transformer winding structure

The equivalent thermal conductivity k_r of the transformer winding in the radial direction is:

$$k_r = \frac{k_1 k_2 d_r}{k_2 d_{r1} + k_1 d_{r2}} \quad (11)$$

Where d_{r1} is the total thickness of the metal conductor in the radial conductor layer of the transformer winding; d_{r2} is the total thickness of the radial oil-impregnated insulating paper of the transformer. d_r is the overall radial thickness of the winding . k_r is the radial equivalent thermal conductivity of the transformer winding; k_1 is the thermal conductivity of metal conductor in conductor layer of transformer winding. k_2 is the thermal conductivity of transformer oil-immersed insulation paper.

The equivalent thermal conductivity k_a of the transformer winding in the axial direction is:

$$k_a = \frac{k_1 k_2 d_a}{k_2 d_{a1} + k_1 d_{a2}} \quad (12)$$

Where d_{a1} is the total thickness of the conductor in the guiding body of the transformer winding shaft; d_{a2} is the total thickness of the axial oil-impregnated insulating paper of the transformer. d_a is the overall axial thickness of winding.

According to the material and structural parameters of the transformer, the equivalent thermal conductivity in each direction of the high and low voltage winding of the transformer is calculated, as shown in Table 4.

Table.4 Equivalent thermal conductivity of transformer windings

Winding direction	Equivalent thermal conductivity / （$W \cdot m^{-1} \cdot K^{-1}$）
Axial direction	0.818
Radial direction	2.096
Direction of wire winding	401

3.3.2 Calculation of equivalent specific heat capacity

The actual oil impregnated insulation paper wrapped on the winding conductor layer can be obtained:

$$c_e m \Delta T = c_1 m_1 \Delta T + c_2 m_2 \Delta T \quad (13)$$

Where c_e is the equivalent specific heat capacity of the transformer winding; m is the total mass of the transformer winding; ΔT is the temperature change of transformer winding. c_1 is the specific heat capacity of conductor layer in transformer winding. c_2 is the specific heat capacity of transformer oil-immersed insulating paper; m_1 is the total mass of conductor layer in transformer winding; m_2 is the total weight of transformer oil-immersed insulation paper. Combined with the material and structural parameters of the transformer, the equivalent specific heat capacity of the low-voltage winding of the transformer is calculated as 398.555 $J \cdot kg^{-1} \cdot K^{-1}$.

3.4. Mesh Independence Study

COMSOL simulation software is used to divide the model. Subsequent simulation calculations are carried out based on COMSOL simulation software. At the same time, mesh independence study is carried out, and hot spot temperatures with different numbers of meshes are given in Table 5. It can be inferred that when the number of nodes is 1909772, the temperature rise reaches a stable value. When stable, the grid diagram is shown in Figure 6.

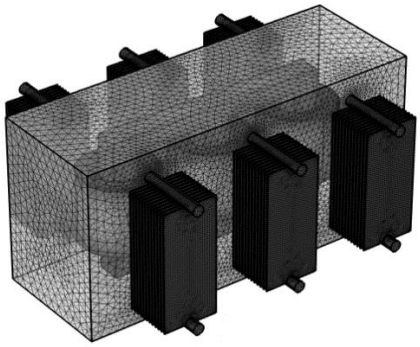

Figure 6. mesh generation

Table 5 The hot spot temperature under different meshes

Number of nodes	1693674	1737481	1793782	1856473	1909772
T_{max}/K	352.2	352.5	352.8	353.3	353.3

3.5. Simulation result analysis

Taking the transformer core and winding losses as heat sources, combined with equivalent thermal parameters of copper wire and insulating paper obtained in Section 3.3, the overall distribution of transformer temperature field and flow field can be obtained through flux-thermal coupling calculation, as shown in Fig. 7 (a)and Fig. 7 (b).

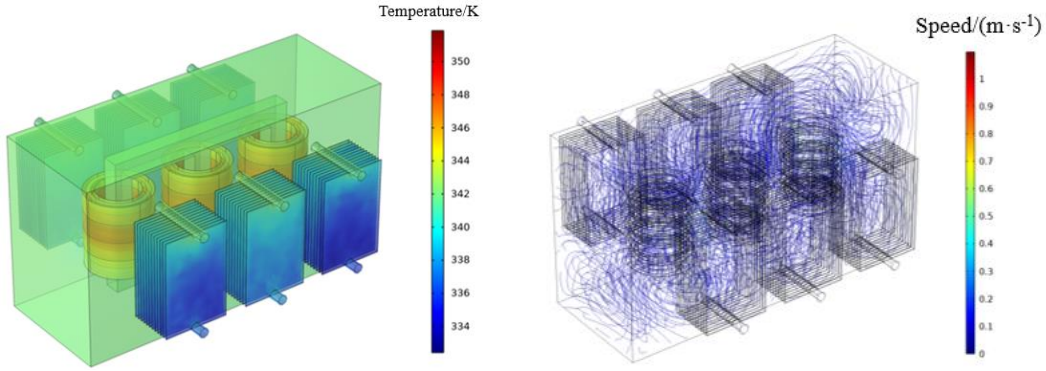

(a) Temperature distribution (b) Velocity distribution

Figure 7. Simulation results of transformer fluid-thermal field

As can be seen from Fig. 6, the temperature distribution law of each winding is basically the same. The hot spot temperature of the transformer is 353.3K, which is located in the middle and upper part of the B-phase winding, mainly due to the poor heat dissipation condition of the B-phase winding. According to the above simulation results, the temperature field distribution results of the B-phase low-voltage winding of the transformer can be extracted, as shown in Fig. 8. As can be seen from the figure, the maximum flow rate is 0.077m/s, the hot spot temperature is 353.3K, and the hot spot temperature is located at the third wire cake in channel 1.

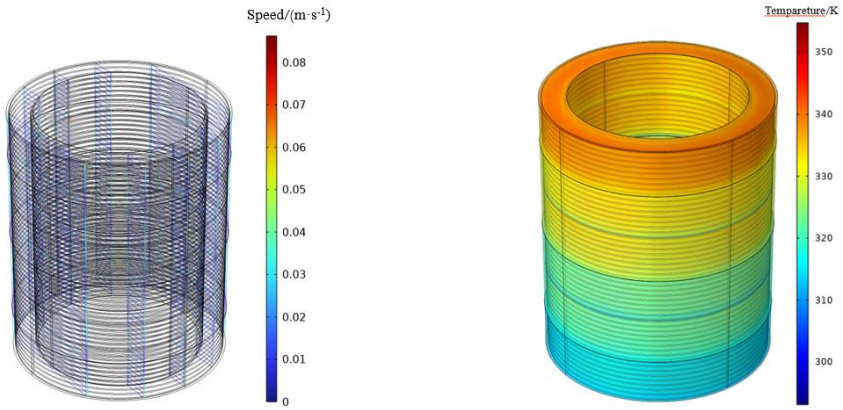

(a) Velocity distribution (b) Temperature distribution

Figure 8. Simulation results of B-phase winding

4. Simulation results of 2D equivalent temperature field of oil-immersed transformer

For the sake of take into account the calculation accuracy and efficiency of thermal field, and consider the subsequent winding optimization design, a 2D equivalent model of low voltage winding of oil-immersed transformer is established.

4.1. 2D transformer equivalent model

In order to obtain the inlet flow rate of the two-dimensional model of the low-voltage winding, a two-dimensional model with the same size as the three-dimensional model of the transformer is constructed, and an oil baffle is built on both sides of the low-voltage winding to make the transformer oil flow into the oil channel of the low-voltage winding, as shown in Fig. 9.

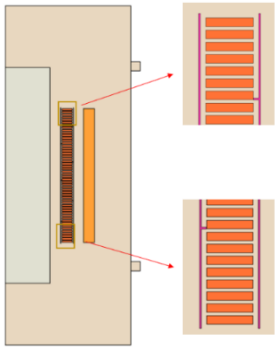

Figure.9 Schematic diagram of transformer 2-D model structure

4.2. Heat sink inlet velocity extraction and simulation results analysis

According to the simulation results of the three-dimensional model, the flow rate of transformer oil flowing from the lower manifold to the bottom of the tank after cooling by the heat sink is extracted, and this flow rate can be used as the inlet boundary condition of the two-dimensional model. The wall where the oil flows from the manifold to the tank is a cross-section, and the average flow rate of the oil flowing through the manifold to the tank area is calculated to be 0.2m/s, as shown in Fig. 10.

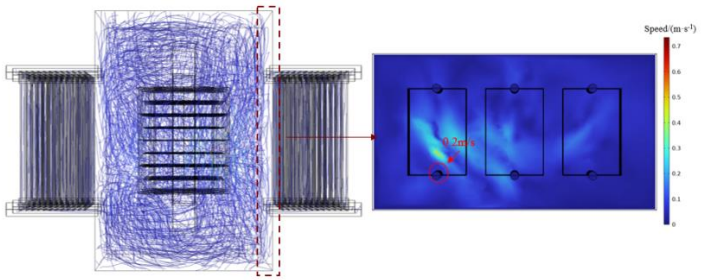

Figure 10. Oil flow velocity distribution in XOZ plane

The inlet velocity at the boundary of the two-dimensional transformer model is set to 0.2 m/s to extract the average oil flow velocity of the transformer oil flowing into the entrance of the low-voltage winding. In Fig. 11, it can be seen that the average flow velocity is 0.05 m/s, which is consistent with the subsequent boundary conditions.

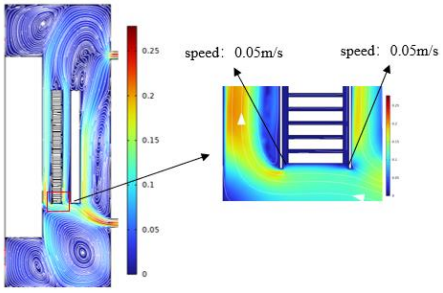

Figure.11 Two-dimensional axisymmetric model of transformer oil flow velocity distribution

The two-dimensional model of the low-voltage winding was constructed, whose dimensions were consistent with the three-dimensional model of the low-voltage winding, including the oil baffle on both sides of the insulation cylinder, which was located on both sides of the vertical oil passage and completely blocked the flow of the oil flow. The detailed geometric parameters had been marked in the figure, as shown in Fig. 12.

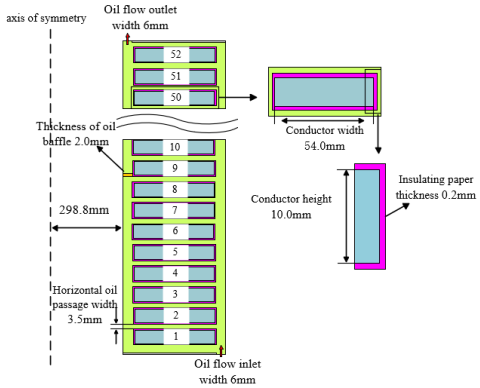

Figure.12 2D schematic diagram of low-voltage winding structure

The extracted inlet flow rate of the low-voltage winding was brought into the two-dimensional model of the low-voltage winding as the boundary condition, and the calculated flow rate distribution and temperature distribution were shown in Fig. 13(a) and Fig. 13(b) respectively.

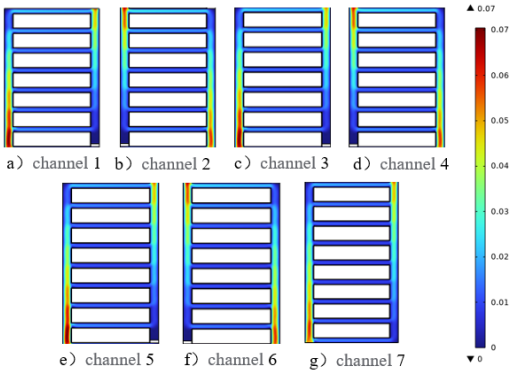

(a) Velocity distribution

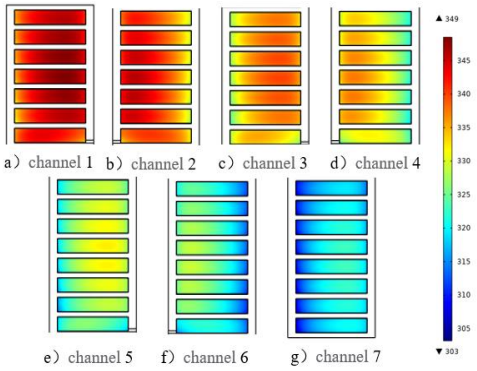

(b) Temperature distribution

Figure 13. Simulation results of 2D winding

It can be seen from Fig. 13(a) and Fig. 13(b) that the maximum flow velocity of oil flow is 0.071m/s. Due to the action of the baffle, the direction of oil flow will change when oil flow passes through the baffle, so the oil flow velocity at the baffle is small, while the oil flow velocity at the entrance of each channel is large. The hot spot temperature of the winding is 348.5K, and the hot spot temperature position is at the fourth wire cake of channel 1. After cooling by the radiator, the oil flow re-enters the oil passage at the entrance, and then diverts through the vertical oil passage to enter each horizontal oil passage. The oil flow after flowing out of the horizontal oil passage is confluent in the vertical oil passage. When flowing through each coil, the oil flow will fully contact the surface of the coil and take away part of the heat, and finally dissipate the heat in the form of heat convection on the surface of the tank wall and the surface of the radiator, thereby reducing the winding temperature.

4.3. Comparison of 2D and 3D simulation results

According to the above simulation results, the overall flow velocity distribution of the two models of the transformer is generally the same, and the maximum flow velocity is 0.071m/s and 0.078m/s, respectively, and the highest flow velocity is located at the entrance of the channel. According to the temperature rise distribution of the low-voltage winding coil cake, the average temperature of 52 coil cakes in the 2D and 3D models was extracted, as shown in Fig.14.

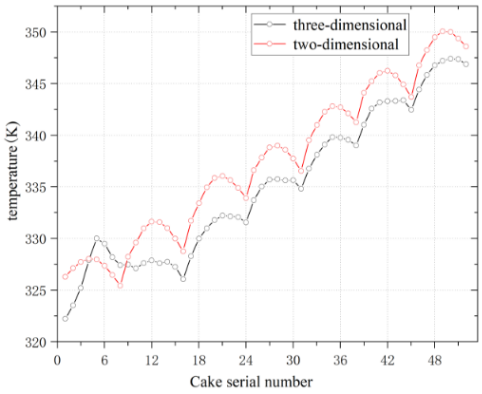

Figure 14. Comparison of average temperature of discs

As can be seen from Fig.14, the overall trend of coil cake temperature is basically the same, and the hot spot temperature of the two-dimensional model and the three-dimensional model is 348.5K and 353.3K respectively, with an error of only 5.98%. Therefore, the three-dimensional thermal field

simulation calculation of the oil-immersed transformer is approximately equivalent to that of the two-dimensional model.

5. Optimization of winding structure parameters of oil-immersed transformer

5.1. Optimization objectives and constraints

In order to reduce the hot spot temperature and conductor consumption of transformer low-voltage winding, considering the influence of winding structure parameters on transformer temperature rise, the winding structure parameters are optimized. In this paper, the following seven parameters that have a certain impact on the winding hot spot temperature are selected as input variables: distance from the low-voltage winding to the core (W_i), conductor cross section length (H_d), conductor cross section width (W_d), inner vertical oil passage width (W_l), outer vertical oil passage width (W_r), horizontal oil passage height (H_1), insulating paper thickness (W_1). The selection of parameters is shown in Fig. 15.

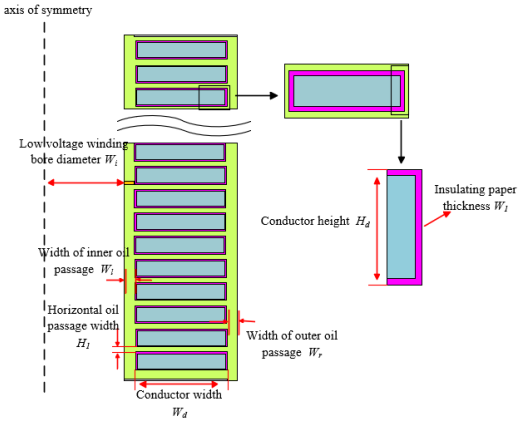

Figure 15. Optimal design variables of winding structure

The allowable range of design variables is determined according to the requirements of the electrical and insulation performance parameters of the oil-immersed transformer. The value range of each structural parameter is shown in Table 6.

Table 6 Design variable range of winding structure parameters

Structural parameter	Value range
Distance between low voltage winding and core W_i/mm	295~315
Traverse height H_d/mm	9~11
Traverse width W_d/mm	42~66
Width of inner vertical oil passage W_l/mm	5~7
Outer vertical oil passage width W_r/mm	5~7
Horizontal oil passage height H_1/mm	3~6
Insulating paper thickness W_1/mm	0~1

The hot spot temperature is calculated by equation (16) in Section 5.4. The calculation method of winding conductor consumption is shown in equation (14), and its value is related to the three parameters of winding W_i, H_d and W_d.

$$V = 52\left[\pi\left(W_i + W_d\right)^2 - \pi W_i^2\right]Hd \tag{14}$$

5.2. Experimental design of Latin Hypercube

The winding losses need to be recalculated and included in the temperature field calculation each time each sample is calculated. Among them, seven variable parameters selected in the paper are adjusted according to the test table, and the other parameters and boundary conditions remain unchanged. According to the Latin Hypercube experimental design method combined with the multi-physics simulation calculation method, the test table shown in Fig.16 can be obtained, and the total number of test design samples is 80.

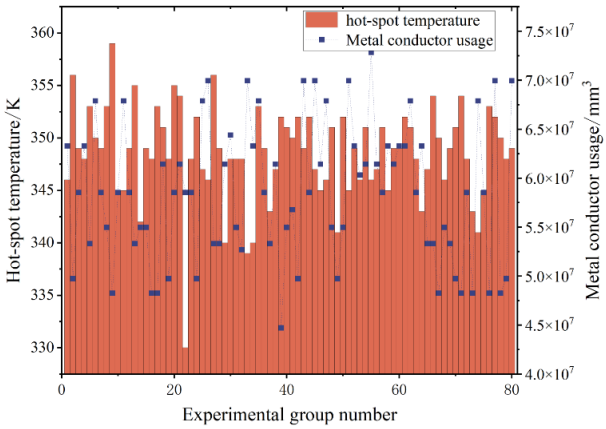

Figure. 16 Latin hypercube experimental design

5.3. Optimized design process

In order to select the structural parameters that make the winding hot spot temperature lowest, the response surface can be used to replace the more complicated model. The optimization design process of this paper is shown in Fig.17.

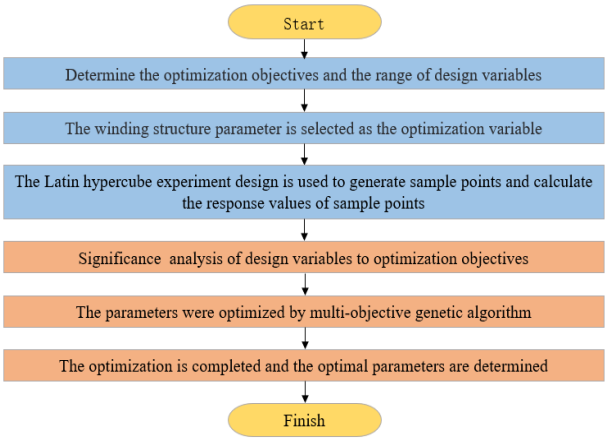

Figure. 17 The Optimization design process

5.4. Hot spot temperature response surface model was established

The response surface function is generally a high-order polynomial function. When the variables are small, the quadratic polynomial can ensure the accuracy of the function and make the model less complicated. In this paper, the quadratic polynomial form is chosen, as shown in equation (15):

$$y = \beta_0 + \sum_{j=1}^{n} \beta_j x_j + \sum_{j=1}^{n} \beta_{jj} x_j^2 + \sum_{i=1}^{n} \sum_{j=i+1}^{n} \beta_{ij} x_i x_j \tag{15}$$

Where, y is the objective function, and β_0, β_j, β_{jj} and β_{ij} are polynomial coefficients, which are also to be evaluated in the response surface model. x_j is the experimental variable; n is the number of experimental variables.

The response relationship is obtained by using the fitting method, as shown in equation (16).

$$\begin{aligned} T_k = {} & 1476.034 - 5.543W_i - 57.462W_l + 14.232W_r \\ & -19.197H_d - 2.184W_d + 11.272H_1 + 75.050W_1 \\ & +0.038W_iW_l - 0.088W_iW_r + 0.002W_iW_d - 0.033W_iH_1 \\ & -0.125W_iW_1 + 4.000W_lW_1 - 0.031W_rW_d - 0.500W_rW_1 \\ & -0.500H_dH_1 - 0.104W_dW_1 - 1.833H_1W_1 + 00095W_i^2 \\ & +2.946W_l^2 + 0.014W_d^2 - 26.216W_1^2 \end{aligned} \tag{16}$$

5.5. Pareto solution set based on NSGS-Ⅱ algorithm

5.5.1 NSGA-Ⅱ optimization algorithm

NSGA-II is a multi-objective genetic algorithm using quick sorting and elite mechanism, which has the characteristics of fast operation speed and good convergence [21-22], and can effectively solve the optimization problem in this paper. The NSGA-Ⅱ optimization algorithm was adopted to optimize the fitted hot spot temperature response surface and the calculated conductor dosage.

5.5.2 Optimization results and simulation verification

The hot spot temperature of transformer winding and conductor consumption were optimized, and the pareto solution set was obtained by NSGA-Ⅱ optimization algorithm, as shown in Fig. 18. Each point corresponds to an optimal solution, and the more dense the solution is, the better the solution is. The points on the front surface can reduce the hot spot temperature and the metal conductor consumption at the same time, but the extreme value cannot be obtained at the same time on the two optimization objectives, and the appropriate optimal solution can be selected according to the actual engineering requirements.

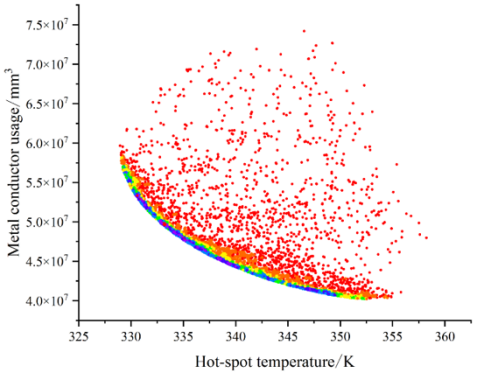

Figure.18 Pareto plots

In order to reduce the hot spot temperature of transformer winding and the metal conductor consumption, two optimization schemes are selected on the Pareto front surface, whose structural parameters are shown in Table 7, and the hot spot temperature and metal conductor consumption calculated on the response surface are shown in Table 8.

Table.7 Winding structure parameter optimization scheme

Design variable	Reference value	Optimization Scheme 1	Optimization Scheme 2
H_1/mm	4.50	4.07	4.26
H_d/mm	10.0	9.58	9.61
W_1/mm	0.5	0.15	0.31
W_d/mm	54.0	51.56	46.62
W_i/mm	305.0	305.72	302.78
W_l/mm	6.0	5.99	6.01
W_r/mm	6.0	6.23	6.11

Tab.8 Results of Pareto optimal designs

Optimization objective	Initial design	Optimization Scheme 1	Optimization Scheme 2
Hot spot temperature /K	348.50	334.04	346.83
Metal conductor usage /mm^3	5.80×10^7	5.08×10^7	4.15×10^7

As can be seen from Table 8, the hot spot temperature of scheme 1 is reduced by 4.16%, and the metal conductor consumption is reduced by 13.79%; the hot spot temperature of scheme 2 is reduced by 0.51%, and the metal conductor consumption is reduced by 28.46%. According to the optimization results, compared with the initial design parameters, all the points on the Pareto front surface can reduce the hot spot temperature and metal conductor consumption. A reasonable Pareto solution can be selected according to the actual engineering requirements, considering the consumption and loss of metal conductors.

6. Conclusion

1) The three-dimensional magnetic-fluid-thermal field simulation model of the oil-immersed transformer was constructed. The distribution of the transformer flow field and temperature field was obtained by finite element simulation software, and the fluid field and thermal field of the low-voltage winding were obtained. The temperature distribution law of each winding was basically the same, and the hot spot temperature of the transformer was 353.3K, located in the middle and upper part of the B-phase winding.

2) A two-dimensional model of transformer low-voltage winding is established, and the distribution of three-dimensional and two-dimensional temperature and fluid fields is compared and analyzed. The maximum flow rates of the two are 0.07045m/s and 0.0776m/s, respectively, which are both at the entrance of the channel. The hot spot temperatures are 348.5K and 353.3K, respectively, and the error is 5.98%, which verifies the accuracy of the two-dimensional equivalent model.

3) The response relation between hot spot temperature and structural parameters is established by response surface method, and the Pareto solution set is obtained by multi-objective optimization algorithm. In order to reduce both the hot spot temperature of the transformer winding and the metal conductor consumption, the hot spot temperature and the metal conductor consumption in scheme 1 are reduced by 4.16% and 13.79% respectively. In scheme 2, the hot spot temperature is reduced by 0.51% and the metal conductor consumption is reduced by 28.46%. The optimization method provides important reference value for guiding the design of oil-immersed transformer.

Acknowledgment

This work is supported by the National Natural Science Foundation of China（52307179）and the Beijing Key of Distribution Transformer Energy-Saving Techonology (China Electric Power Research Institute) (PDB51202301652).

Nomenclature

C_e —The equivalent specific heat capacity of the transformer winding, [J·kg^{-1}·K^{-1}]

C_p — The heat capacity at constant pressure, [J·kg^{-1}·K^{-1}]

F — External force per unit volume, [N/m^3]

g — Gravitational acceleration, [m/s^2]

h — Convective heat transfer coefficient, [W·m^{-2}·K^{-1}]

J_s — The current density of the winding, [A/m^2]

k — The thermal conductivity, [W·m^{-1}·K^{-1}]

k_r — The radial equivalent thermal conductivity, [W·m^{-1}·K^{-1}]

k_a — The axial equivalent thermal conductivity, [W·m^{-1}·K^{-1}]

p — Fluid pressure, [N/m^2]

q — The heat source density of structural parts, [W/m^3]

Q — Heat source per unit volume, [W/m^3]

T — Temperature, [K]

V — Velocity, [m/s]

Greek symbols

ρ — Solid density, [kg/m^3]

ρ_0 — Fluid density, [kg/m^3]

∇ — Hamiltonian operator

σ — The electrical conductivity, [S/m]

μ — Magnetic permeability, [H/m]

μ_0 —Hydrodynamic viscosity, [N·S/m^2]

λ — The thermal conductivity, [W/(m·K)]

References

[1] Joachim S, et al., Asset management techniques, International Journal of Electrical Power and Energy Systems, 28(2006), pp. 643-654.

[2] Zhang S.L., et al., Lumped RC thermal network Method applied to oil and gas casing transient temperature calculation, High Voltage Engineering, 41 (2015), 07, pp. 2294-2301.

[3] Kim J K, et al., Compact thermal network model of the thermal interface material measurement apparatus with multi-dimensional heat flow, IEEE Transactions on Components, Packaging and Manufacturing Technology, 1(2011), 8, pp. 1186-1194.

[4] Tang Z., et al., Simulation Analysis of Thermal network model of Dry Transformer considering Fluid Dynamics , Transactions of China Electrotechnical Society, 37(2022), 18, pp. 4777-4787.

[5] Wang Q.Y., et al., 3- D coupled electromagnetic-fluid-thermal analysis of epoxy impregnated paper converter transformer bushings, IEEE Transactions on Dielectrics and Electrical Insulation, 24(2017), 1, pp. 630-638.

[6] Liao C.B., et al., 3-D coupled electromagnetic-fluid-thermal analysis of oilimmersed triangular wound core transforme, IEEE Transactions on Magnetics, 50(2014), 11, pp. 1-4.

[7] Liu C., et al. Temperature rise of a dry-type transformer with quasi3D coupled-field method, IET Electric Power Applications, 10(2016), 7, pp. 598-603.

[8] Hu W.J., et al., Research on Calculation Method of Steady-State Temperature Rise and Step Reduction for Oil-Immersed Power Transformer Windings, Proceedings of the CSEE, 43(2023), 16, pp. 6505-6517.

[9] Luo R.S., et al. Three-dimensional Temperature Rise Calculation and Optimal Design Method of High Power High Frequency Transformer, Transactions of China Electrotechnical Society, 38(2023), 18, pp. 4994-5005+5016.

[10] Lu J.C., et al. Simplified hot spot calculation of 35 kV oil-immersed transformer based on porous media theory, High Voltage Engineering, pp. 1-10.

[11] Liu G., et al. Research on node data mapping algorithm for the 2D coupling electromagnetic-fluid-thermal fields, Transactions of China Electrotechnical Society, 33(2018), 1, pp, 148-157.

[12] Li D.J., Temperature Field Analysis of Oil-immersed Transformer and Influence Factors of Oil Flow on Internal Temperature Rise, MSc thesis, Southwest Jiaotong University, Chengdu, 2013.

[13] Huang J., Study on the Influence of Oil Flow on the temperature rise of Oil-immersed transformer winding horizontal oil Passage, MSc thesis, Kunming University of Science and Technology, Kunming, 2019.

[14] Li L., et al. Analysis of influencing factors of temperature rise of cracked windings in oil-immersed power transformers, Electric Power Automation Equipment, 36(2016), 12, pp. 83-88.

[15] Liao C.B., et al. Three-dimensional electromagnetic, fluid-temperature Field Coupling Analysis Method for Oil-Immersed Transformer, Electric Power Automation Equipment, 35(2015), 09, pp. 150-155.

[16] Zhou L.J., et al. Thermal modelling and hot spot locating for transformer winding in oil forced and directed cooling mode, High Voltage Engineering, 46(2020), 11, pp. 3896-3904.

[17] Liu G., et al. Two-dimensional temperature field analysis of oil-immersed transformer based on non-uniformly heat source, High Voltage Engineering, 43(2017), 10, pp. 3361-3370.

[18] Yuan F.T., et al. Temperature characteristics analysis of oil-immersed transformer and heat sink optimization based on multi-physical field simulation, High Voltage Engineering :1-12

[19] Yuan F.T, et al. Thermal optimization for nature convection cooling performance of air core reactor with the rain cover, IEEJ Transactions on Electrical and Electronic Engineering, 13(2018), pp. 1-9.

[20] Eslamian M., et al. Thermal analysis of cast-resin dry-type transforemrs, Energy Conversion and Management, 52(2011), pp. 2479-2488.

[21] Liao C.B., et al. 2-D coupled electromagnetic-fluid-thermal analysis of oil-immersed transformer, Science Technology and Engineering, 36(2014), 14, pp. 67-71.

[22] Multi-objective optimization using nondominated sorting in genetic algorithms[J]. Evolutionary Computation, 2(1994), 3, pp. 221-248.

[23] Yuan F., et al. Optimization design of oil-immersed iron core reactor based on the particle swarm algorithm and thermal network model, Mathematical Problems in Engineering, 2021(4): 1-14.

Paper submitted: 25.01.2024

Paper revised: 18.04.2024

Paper accepted: 24.04.2024